

## NMR Diffusion Measurements of Complex Systems

*Tim Stait-Gardner, Scott A. Willis, Nirbhay N. Yadav, Gang Zheng, and William S. Price*

College of Health and Science, University of Western Sydney, Australia

Corresponding author:

William S. Price

College of Health and Science

University of Western Sydney

Locked Bag 1797, Penrith South DC, NSW 1797, Australia

E-Mail: w.price@uws.edu.au

### Abstract

The pulsed gradient spin-echo nuclear magnetic resonance experiment is a powerful tool for studying the constitution and structure of complex systems (e.g., polydisperse systems and porous media). In applications to polydisperse systems, it is important to consider the effects of obstruction, exchange, entanglement, and diffusional averaging processes whereas in applications to porous samples, reliable structural information can only be extracted from the time-dependence of the apparent diffusion coefficient when the deleterious effects of spatially and/or temporally inhomogeneous background (magnetic field) gradients can be suppressed. These issues are considered in this review.

### Keywords

Self-diffusion, restricted diffusion, NMR, PGSE, porous, polydisperse, background gradient

### 1. Introduction

Nuclear Magnetic Resonance (NMR) is the most powerful non-invasive technique for probing self-diffusion. Combining this with the ease of sample preparation and the range of systems that may be investigated makes for a very attractive technique. Self-diffusion refers to diffusion occurring in a system at equilibrium, thus the diffusion coefficient of pure H<sub>2</sub>O is a measurement of self-diffusion as is the diffusion coefficient of ethanol in a homogenous water-ethanol solution. Contrast this with mutual-diffusion which takes place in a system approaching equilibrium via a chemical potential gradient. NMR is ideal for measuring self-diffusion coefficients [1-3]. Other methods for measuring diffusion such as using radio tracers are better suited for measuring mutual diffusion. The range of diffusion coefficients that may be probed by NMR span over seven orders of magnitude, ranging between  $10^{-7} \text{ m}^2\text{s}^{-1}$  to  $10^{-14} \text{ m}^2\text{s}^{-1}$  (and comfortably beyond in favourable samples).

Starting with the basic theory of NMR based diffusion measurements this chapter then proceeds to demonstrate the wide range of systems in which diffusion may be investigated using this powerful and versatile technique. After introducing the pulsed

gradient spin-echo (PGSE) technique for measuring diffusion (a standard two pulse sequence) some applications of this sequence (and simple variants thereof) to investigating complex systems are examined. These include discussion of some diffusional averaging processes that occur in polydisperse macromolecular solutions and changes in the apparent diffusion coefficient due to geometrical confinement. In these more complex applications of the PGSE sequence the deleterious effects of unwanted background gradients become apparent. Thus the chapter concludes with a discussion on more complex variants of the basic PGSE sequence which enable the reduction of background gradient effects.

## **2. Pulsed Gradient Spin-Echo (PGSE) NMR**

The PGSE NMR sequence for measuring translational diffusion will be described in moderate detail. More detail can be found in Refs. [2, 4-7]. An understanding of the simple Hahn-echo based PGSE sequence provides a good basis for understanding the capabilities of NMR diffusion in general. The most appropriate sequence to use depends upon the nature of the system under study.

It is assumed that not all readers are familiar with NMR so the basics needed for understanding the PGSE sequence will be covered now. Many nuclei (such as  $^1\text{H}$ ,  $^2\text{H}$  and  $^{13}\text{C}$ ) have a magnetic moment and in effect behave like little bar magnets (ignoring some of the more subtle points in quantum mechanics). The strength of the nuclear magnetism decreases as the mass of the nucleus increases thus the most NMR sensitive nucleus is the proton ( $^1\text{H}$ ). A sample is of macroscopic dimension and is composed of a number of nuclei on the order of Avogadro's number. Normally the magnetic moments of the nuclei are distributed randomly and there is no net macroscopic magnetisation. If the sample is placed in a strong magnetic field the magnetic moments of the nuclei will have a slight preference to align along the field in the same manner that a compass needle has a preference to align north (the preference is slight as the molecules are all in thermal motion). The result is a macroscopic magnetisation (arising from the nuclei) aligned along the field. This is illustrated in Fig. 1A. An NMR spectrometer has a large magnetic field (11.74 T say) in which the sample is placed. The spectrometer can manipulate this macroscopic magnetisation by means of radiofrequency (RF) pulses and magnetic gradient pulses.

RF pulses can be used to manipulate the macroscopic magnetisation by rotating it. Nuclear species have different magnetic moments, and different frequency RF pulses will rotate different components of the macroscopic magnetisation (belonging to different nuclei). Only one nuclear species is needed to measure diffusion ( $^1\text{H}$  is chosen here). The RF pulses used to manipulate the magnetisation last on the order of a few microseconds. One of the most common manipulations is to flip the magnetisation onto the horizontal plane so that it is  $90^\circ$  to the magnetic field (see Fig. 1B).

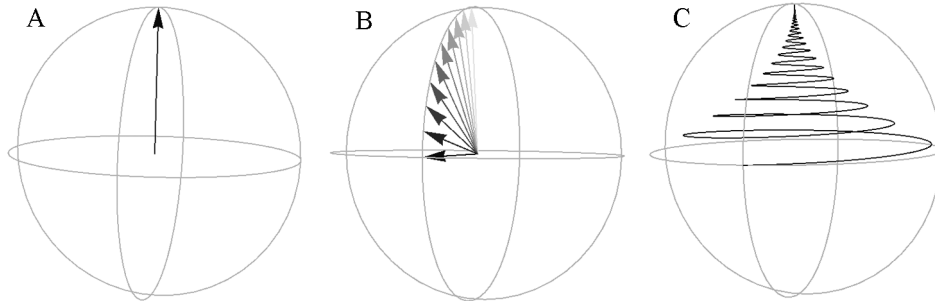


Fig. 1: The magnetic field is aligned vertically. (A) The equilibrium magnetisation points along the field. (B) An RF pulse can be used to rotate the magnetisation from the vertical to the horizontal as illustrated here. The RF pulse only lasts on the order of a few microseconds. The magnetisation, once perturbed in this manner, will begin to relax back to equilibrium. (C) The evolution of the magnetisation after a  $90^\circ$  RF pulse for some “typical” parameters. Note that the relaxation process typically takes over two orders of magnitude longer to return to equilibrium than the RF pulse took to perturb the magnetisation to the transverse state.

Once the magnetisation is perturbed from the vertical it will begin to relax back to equilibrium. Two processes take place during its evolution: it will precess about the main magnetic field with a frequency known as the Larmor frequency ( $\sim 500$  MHz for a proton in an 11.74 T magnetic field); it will also realign with the main magnetic field returning to equilibrium (a process quantified by two parameters describing the longitudinal and transverse relaxation). Note that the Larmor frequency is proportional to the magnetic field strength and is described quantitatively as

$$\omega = -\gamma(B_0 + \mathbf{g} \cdot \mathbf{r}), \quad (1)$$

where  $\gamma$  is the gyromagnetic ratio, a constant for each nucleus (for protons  $\gamma = 267.522 \times 10^6 \text{ rad s}^{-1} \text{ T}^{-1}$ ) [8],  $B_0$  is the magnitude of the static magnetic field,  $\mathbf{g}$  is the gradient and  $\mathbf{r}$  is position.

The evolution of the magnetisation by showing the trajectory of the tip of the arrow during a “typical” relaxation process is illustrated in Fig. 1C. The NMR spectrometer can acquire a signal by opening its receiver channel. The precessing magnetisation induces a current in the receiver via Faraday induction. This signal is called the free induction decay (FID) and is proportional to the transverse component of the magnetisation and has the appearance of a sine wave enveloped by a decaying exponential. There is much information that can be stored in the FID (the FID is usually Fourier transformed to yield a spectrum for analysis) but for measuring self-diffusion its magnitude at the initial point of acquisition is all that is needed.

A measurement of diffusion requires that the molecules be labelled in some way so their motion can be traced. In NMR a spatially dependent magnetisation is created within the sample and from observations of its evolution over time the diffusion coefficient of the molecules of interest can be inferred. Gradient pulses are used to create the spatially dependent magnetisation. To see how the gradient pulses work recall that the Larmor frequency is proportional to the magnetic field strength. A constant gradient will result in

a linear variation in the magnetic field. Consider the gradient to be aligned along the  $z$ -direction (other directions can be useful, for example, in situations where the diffusion is anisotropic). The NMR sequence used to illustrate diffusion measurement in this section is the PGSE sequence which is shown in Fig. 2A. Often it is assumed that the only magnetic gradient that must be considered is the purposely applied one (i.e.  $g = g_a$ ). However, sometimes the presence of a background gradient  $g_0$  must also be accounted for (see Section 5).

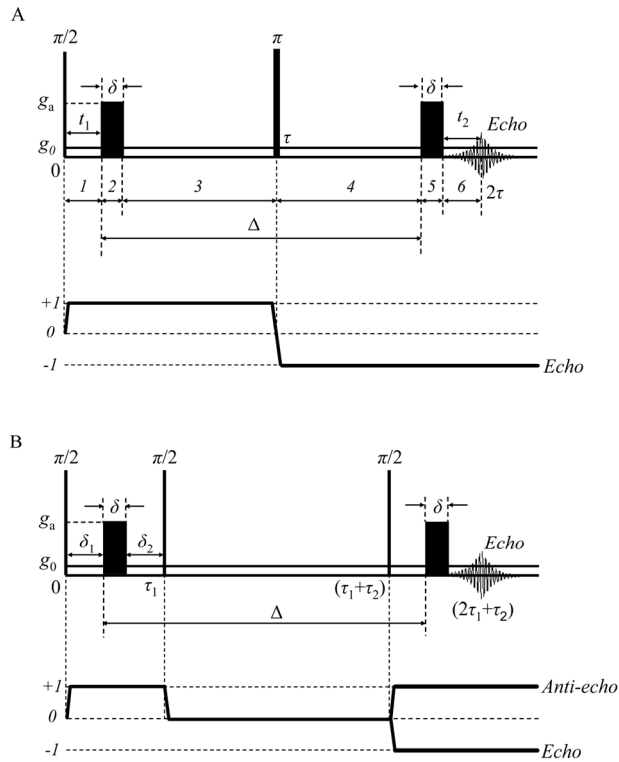


Fig. 2: The Hahn spin-echo PGSE sequence (A) and the stimulated echo-based PGSE sequence (STE-based PGSE) (B). For the Hahn spin-echo PGSE sequence, two pulsed gradients of duration  $\delta$  and magnitude  $g_a$  are inserted into each  $\tau$  delay; for the STE-based PGSE sequence, two pulsed gradients of duration  $\delta$  and magnitude  $g_a$  are applied in the two encoding intervals,  $(0$  to  $\tau_1)$  and  $(\tau_1 + \tau_2$  to  $2\tau_1 + \tau_2)$ , which are separated by the phase storage period ( $\tau_2$ ). It is assumed that the background gradient is constant during the pulse sequences and has a magnitude of  $g_0$ . The separation between the leading edges of the pulsed gradients is denoted by  $\Delta$  (i.e., observation time or diffusion time). The applied gradient is along the  $z$ -axis (the direction of  $\mathbf{B}_0$ ). The Hahn spin-echo-based PGSE sequence can be divided into 6 intervals according to the variation of the net magnetic gradients. Only the second half of the echo is digitised and used as the free induction decay (FID). The coherence pathways are also shown here. The STE-based PGSE sequence only captures half the magnetisation that the Hahn spin-echo PGSE sequence does.

Immediately after the  $90^\circ$  RF pulse the magnetisation is flipped to the  $xy$ -plane as indicated in Fig. 1B. Looking at how it varies along the  $z$ -axis after the first RF pulse the magnetisation appears as illustrated in Fig. 3A (note that there is still no spatial dependence and the magnetisation is considered to be only a function of  $z$ ). Following the RF pulse is a short period of precession during which the magnetisation still appears much as in Fig. 3A. Following this the magnetisation is wound up into a helix during the finite length of the gradient pulse (i.e. it picks up a spatially dependent phase during the gradient pulse until it appears as illustrated in Fig. 3B). This occurs because there is a linear variation in the magnetic field and thus a linear variation in the Larmor frequency with respect to position along the  $z$ -axis.

There is a period of free precession until the application of the next gradient pulse after a delay  $\Delta$  (the time between the leading edges of the gradient pulses). A  $180^\circ$  pulse is applied to change the handedness of the magnetisation helix (see Fig. 3C) so that the second gradient pulse unwinds the helix as opposed to winding it up further. It might be asked why the  $180^\circ$  pulse is not left out of the sequence and the second gradient pulse replaced with a negative gradient so as to simplify the sequence. Indeed this will work in some cases but is far from ideal since the  $180^\circ$  RF pulse also cancels out some other effects (chemical shift evolution) and thus makes for a better sequence – indeed it refocuses magnetisation with varying Larmor frequency at the point of acquisition.

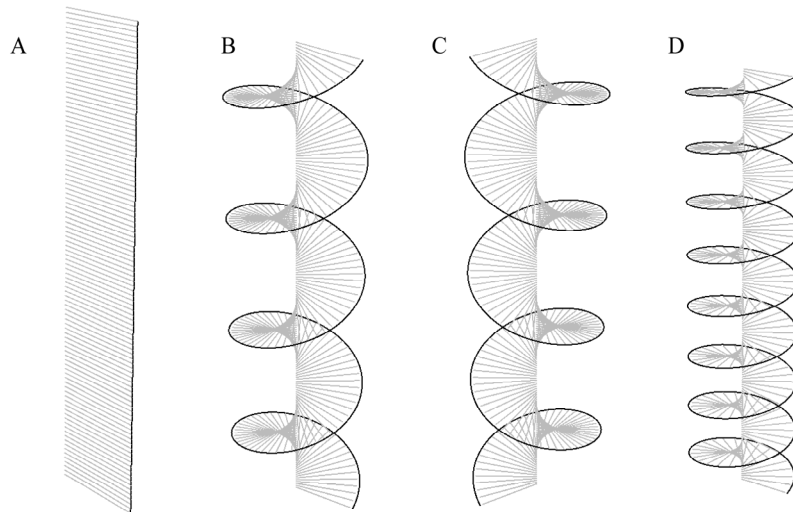


Fig. 3: (A) The magnetisation after the  $90^\circ$  RF pulse. The magnetisation will also appear like this after the short period a precession (although it will have relaxed a little and may have a small longitudinal component). (B) A spatial variation in magnetisation is created by application of a gradient pulse. This is how the magnetisation appears after application of the gradient pulse. (C) The  $180^\circ$  pulse inverts the handedness of the magnetisation helix (compare to Fig. 3B). (D) More finely pitched helices (compare with Fig. 3B) attenuate more quickly as a result of diffusion because the molecules carrying the magnetisation do not have to move as far relative to each other to start to significantly cancel each other's magnetisation.

The magnetisation is carried by the molecules composing the sample. These molecules are in constant thermal motion. This self-diffusion serves to attenuate the magnetisation helix as molecules that start out initially close to each other with nuclei with similar magnetic moment orientations move away from each other into regions where the magnetic moment orientations differ. The second gradient pulse unwinds the magnetisation such that a signal can be acquired. The magnetisation helix not only attenuates as a result of diffusion but also as a result of the other relaxation processes alluded to earlier (recall that when perturbed from equilibrium the magnetisation undergoes a trajectory similar to that given in Fig. 1C in returning to equilibrium). Thus it is not enough to measure the magnitude of the FID at acquisition to obtain the diffusion coefficient since this magnitude has also been affected by other attenuating processes. A number of measurements must be made (the minimum is two but more is better) using a variety of differently pitched magnetisation helices (see Fig. 3B and Fig. 3D). Diffusion will affect the attenuation of these helices differently. In a finely pitched helix for example, the molecules will not have to move very far for them to have migrated into a region with a very different magnetisation phase and thus diffusion will cause more rapid helix attenuation in this case. In coarsely pitched helices the molecules have to move quite far from their starting positions before they begin to significantly cancel each other's magnetisation and thus these helices attenuate slowly as a result of diffusion. The other attenuation processes (those caused by relaxation) do not depend upon position and affect all helices equally. Differently pitched magnetisation helices can be created by repeating the experiment and incrementing the gradient strength  $g$  while leaving the other parameters unaltered.

One way of quantifying the helix pitch is via the parameter  $q$  which quantifies the number of revolutions in the magnetisation helix per unit distance and is given by  $q = \gamma g \delta / 2\pi$  ( $\text{m}^{-1}$ ) where  $\delta$  is the duration of the gradient pulse. Typical values of  $g$  (e.g., between  $0.027 \text{ T m}^{-1}$  and  $0.43 \text{ T m}^{-1}$  for a high resolution gradient NMR probe) and  $\delta$  (1 ms) used during the measurement of the diffusion coefficient of water result in  $q$  values between  $1150 \text{ m}^{-1}$  and  $18300 \text{ m}^{-1}$  – that is the helices have between approx. 11 and 180 revolutions per centimetre. The diffusion coefficient of residual HDO in  $\text{D}_2\text{O}$  is  $D = 1.902 \times 10^{-9} \text{ m}^2 \text{ s}^{-1}$  [9]. The diffusion coefficient is related to the mean square displacement of a molecule by [10]

$$\langle (\mathbf{r}' - \mathbf{r})^2 \rangle = \int_{-\infty}^{\infty} \int_{-\infty}^{\infty} (\mathbf{r}' - \mathbf{r})^2 \rho(\mathbf{r}) P(\mathbf{r} | \mathbf{r}', \Delta) d\mathbf{r} d\mathbf{r}' \quad (2)$$

where  $\rho(\mathbf{r})$  is the spin density and  $P(\mathbf{r} | \mathbf{r}', \Delta)$  is the probability of a molecule moving from  $\mathbf{r}$  to  $\mathbf{r}'$  during  $\Delta$ . In a free homogenous isotropic solution Eq. (2) gives

$$\langle (\mathbf{r}' - \mathbf{r})^2 \rangle^{1/2} = \sqrt{6Dt} \quad (3)$$

where  $\langle (\mathbf{r} - \mathbf{r}')^2 \rangle^{1/2}$  is the root mean square (RMS) displacement and  $t$  is time. On a time scale of 100 ms a RMS displacement for a water molecule of  $33.8 \mu\text{m}$  is expected. For  $q = 11.5 \text{ cm}^{-1}$  this is only  $1/25^{\text{th}}$  of a revolution of its magnetisation and so only minimal diffusive attenuation should occur during 100 ms. For the  $q$  value of  $183 \text{ cm}^{-1}$  the RMS

displacement of a water molecule corresponds to about 1.6 cycles of the magnetisation helix and thus a significant attenuation of this magnetisation helix as a result of diffusion is expected.

The Stejskal-Tanner equation exactly quantifies the diffusive attenuation resulting from application of the PGSE sequence. The signal strength depends upon  $\gamma$ ,  $\delta$ ,  $g$ ,  $\Delta$  (most of the diffusive attenuation takes place during this period), and finally  $D$ . Many of these parameters appear in Fig. 2A. The Stejskal-Tanner equation is

$$\begin{aligned} E(q, \Delta) &= S^{t=acq} / S_{g=0}^{t=acq} = \exp\left(-D\gamma^2 g^2 \delta^2 (\Delta - \delta/3)\right) \\ &= \exp\left(-4\pi^2 Dq^2 (\Delta - \delta/3)\right) \\ &= \exp(-bD). \end{aligned} \quad (4)$$

where  $t = acq$  is the acquisition time, with  $b$  the term including all of the delays, gradient strength and gyromagnetic ratio for the pulse sequence used.  $S^{t=acq} / S_{g=0}^{t=acq}$  is the normalised signal at the time of acquisition (the signal strength with the gradient divided by the signal strength without the gradient). This normalisation allows for the removal of relaxation attenuation.

All the parameters on the right hand side of Eq. (4) are known except  $D$ . By incrementing the gradient  $g$  and measuring the signal strength, Eq. (4) can be fitted to the data to determine  $D$ . Putting the  $q$  values of  $11.5 \text{ cm}^{-1}$  and  $183 \text{ cm}^{-1}$  into Eq. (4) and using  $D = 1.902 \times 10^{-9} \text{ m}^2 \text{ s}^{-1}$  (residual HDO in  $\text{D}_2\text{O}$ ), the normalised signal  $S^{t=acq} / S_{g=0}^{t=acq}$  is found to be 0.99 (that is 99% as strong as it would have been without a gradient) and 0.08 (that is only 8% as strong as it would have been without a gradient) respectively. Eq. (4) thus predicts the behaviour that is expected (based on the calculations using Eq. (3) given earlier). Eq. (4) has not been derived here but a brief discussion of how it can be derived will now be given (see also Eq. (23)).

The discussion about the workings of the PGSE sequence has been qualitative in the lead-up to Eq. (4). Mathematically the macroscopic magnetisation obeys the Bloch equation [11]

$$\frac{d\mathbf{M}(t)}{dt} = \gamma \mathbf{M} \times \mathbf{B}(t) - \frac{M_x \mathbf{i} + M_y \mathbf{j}}{T_2} - \frac{(M_z - M_0) \mathbf{k}}{T_1}, \quad (5)$$

where  $\mathbf{B}(t)$  is the magnetic field vector,  $M_x$  and  $M_y$  are the components of the magnetisation in the  $x$  and  $y$  directions, respectively,  $M_0$  is the magnitude of the equilibrium magnetisation (aligned along the  $z$ -axis) and  $\mathbf{i}$ ,  $\mathbf{j}$  and  $\mathbf{k}$  are unit vectors pointing along the  $x$ ,  $y$  and  $z$  axes, respectively. These equations depend only upon the magnetisation at a point and not at all on neighbouring points. Ignoring the evolution given by Eq. (5) the magnetisation should be expected to evolve in time via diffusion. This is described by the standard diffusion equation

$$\frac{\partial \mathbf{M}}{\partial t} = D \nabla^2 \mathbf{M}. \quad (6)$$

Combining the two forms of time evolution quantified by Eqs. (5) and (6) results in the Torrey-Bloch equation [12]

$$\frac{\partial \mathbf{M}(\mathbf{r}, t)}{\partial t} = \gamma \mathbf{M} \times \mathbf{B}(\mathbf{r}, t) - \frac{M_x \mathbf{i} + M_y \mathbf{j}}{T_2} - \frac{(M_z - M_0) \mathbf{k}}{T_1} + D \nabla^2 \mathbf{M}. \quad (7)$$

By tracing the magnetisation through the PGSE sequence given in Fig. 2A using the Torrey-Bloch equation (Eq. (7)) Eq. (4) can be derived explicitly [5, 13].

### 3. Diffusion in Freely Diffusing Macromolecular Systems

The signal attenuation from an NMR diffusion experiment for a freely diffusing species is in the form of an exponential decay and when there is only one diffusion coefficient present (i.e. a monodisperse sample) this decay is monoexponential (i.e. one exponential decay constant). While natural polymers (e.g. proteins) are usually monodisperse [14, 15], synthetic polymers may be very polydisperse (i.e. there is a molecular weight distribution) and this makes the diffusion in these systems difficult to model. Diffusion in polydisperse macromolecular solutions is affected by phenomena such as obstruction and entanglement and these effects are averaged for the diffusion time as they generally occur on a smaller timescale than the measurement [2, 16]. Obstruction by the larger molecules in a polydisperse system results in a reduction in the diffusion coefficient of the smaller molecules (self-obstruction also occurs and results in a reduced diffusion coefficient) and different mathematical models are available [15, 17]. These models are, however, oversimplifications because of the assumptions they make [16, 18]. Consider the results of using two such models in a protein aggregation study by Price *et al.* [15]. Further complication arises if it is a polydisperse system of aggregate species since the aggregations may have different lifetimes [16].

Non-linearity in the logarithmic attenuation plots should be noticeable even for very low polydispersities [19, 20], but this is often not seen and the resulting plots are often linear or the non-linearity is reduced (even for higher polydispersities) [15, 21]. Even for simple bimodal mixtures of polymers, although the logarithmic attenuation plots are non-linear, they are closer to linear than predicted [19]. Hence, two other diffusional averaging processes – macroscopic and microscopic (ensemble) averaging – are often discussed in the literature. The former is the ability to describe the attenuation by the component diffusion coefficients and their population fraction in the polydisperse system [19]. The latter is used to describe the deviation from the macroscopic average [16, 19, 21] and is seen as a narrowing of the distribution of the diffusion coefficients [16, 19, 22].

#### *Understanding polymer solutions*

When studying polymer solutions (and before dealing with the problems associated with polydispersity) it is important to understand that the diffusive behaviour may be

dependent on the concentration range (e.g. dilute – semi-dilute – concentrated), in particular the overlap concentration(s) (where the polymers start to interact and then eventually entangle) may need to be considered (for example see Refs. [23-31]). It is also common to come across theories like that of reptation [29, 30, 32-34] (the forced curvilinear (snake-like) motion of a linear polymer due to entanglement making a fixed tube for motion), constrained release [29, 30, 32-34] (the tube created by the entanglement only dampens the lateral movement of the linear polymer because the entanglement is fluid (a tube renewal process)) and arm retraction [35, 36] (branched polymers cannot undergo reptation in one direction (arm retraction then core hopping)).

To assist with modelling diffusion in polymer systems empirical scaling laws are often available or observed. Such scaling laws show how a property such as diffusion depends on the concentration, molecular weight or both (for examples see Refs. [21, 26, 31, 37-42]). It is common to find the relation between molecular weight and diffusion as [20, 22, 38, 42, 43],

$$D = kM^{-\beta} \quad (8)$$

where  $M$  is the molecular weight and  $k$  and  $\beta$  are constants that depend on the type of polymer and solvent parameters. However, such scaling laws are only a guide and may only be applicable to certain molecular weight ranges since the scaling laws may not take into account shape changes as the molecular weight increases (rods to random coils, for example) [44].

#### *Diffusion and the effect of a molecular weight distribution*

The polydispersity index (PDI) provides a means of characterising polydispersity [14],

$$\text{PDI} = \frac{\overline{M}_w}{\overline{M}_n} \quad (9)$$

where  $\overline{M}_n$  is the number-average molecular weight,  $\overline{M}_w$  is the weight-average molecular weight. Some consider a PDI < 1.1 to be the critical value for defining monodisperse polymers [14], while those with a PDI ≤ 1.25 are narrow polydispersity polymers [45]. Fractionated polymers fall in the range of 1.30 ≤ PDI ≤ 1.75 and polymers with a PDI between 1.8 and 2.4 are poorly fractionated [45]. Wide distribution polymers have a PDI ≥ 2.5 [45] with some commercial polymers having a PDI of up to 30 [14].

The molecular weight of a polydisperse polymer can be expressed in a number of ways [14, 19-21, 43, 46, 47], and the average molecular weight value measured for a polydisperse polymer depends on the technique used to measure it [14]. The full molecular weight distribution can be measured with techniques such as gel permeation chromatography [47, 48]. Diffusion measurements give a diffusion-average molecular weight,  $M_D$  [20, 43, 46], the value of which depends on the technique used to measure it and the concentration of the solution for which the diffusion was measured. In order to see how the diffusion-average molecular weight comes about (for a discrete polydisperse system or a system of different size ‘permanent’ aggregates where the NMR signals are the same or overlapped) we must consider the signal and its attenuation. The NMR signal

(and its attenuation) is now a sum of the contributing signals and so [15, 16, 19-21, 37, 49],

$$S_g^{t=acq} = \sum_i S_{i, g=0 \text{ T m}^{-1}}^{t=acq} E_i \quad (10)$$

where  $i$  represents the number of components in the system. Rewriting Eq. (10) to show the net equilibrium magnetisation ( $M_{0, i}$ ), the relaxation term ( $\exp(R_i)$ ) and the diffusion term ( $\exp(-bD_i)$ ) we get

$$S_g^{t=acq} = \sum_i M_{0, i} \exp(R_i) \exp(-bD_i) \quad (11)$$

but since the net equilibrium magnetisation relates to the number (or amount, i.e. moles),  $n$ , and the molecular weight of component  $i$  then

$$S_g^{t=acq} = \sum_i M_i n_i \exp(R_i) \exp(-bD_i). \quad (12)$$

The next step is to consider if the relaxation term can be neglected for the particular system or molecular weights present. It is often deemed independent of molecular weight [15, 16, 19-21], although it should be considered for any study since variations of the relaxation times with molecular weight may give ‘diffusion time’ dependent attenuation [20]. However neglecting relaxation and normalising the attenuation data to the signal when  $g = 0 \text{ T m}^{-1}$ , Eq. (12) becomes

$$E = \frac{S_g^{t=acq}}{S_{g=0 \text{ T m}^{-1}}^{t=acq}} = \frac{\sum_i M_i n_i \exp(-bD_i)}{\sum_i M_i n_i} \quad (13)$$

and this leads to the weighted average diffusion coefficient [15, 16, 21],

$$\langle D \rangle_w = \frac{\sum_i M_i n_i D_i}{\sum_i M_i n_i}. \quad (14)$$

Using Eq. (8) and Eq. (14) the weighted average diffusion coefficient can be expressed in terms of the diffusion-average molecular weight [20, 43, 46],

$$\langle D \rangle_w = k_D M_D^{-\beta_D} \quad (15)$$

where  $k_D$  and  $\beta_D$  represent the coefficients of the scaling law for the weighted average diffusion coefficient. So from Eq. (14), Eq. (15) and again Eq. (8),

$$M_D = \frac{1}{k_D} \left( \frac{\sum_i M_i^{1-\beta} n_i k_i}{\sum_i M_i n_i} \right)^{\frac{1}{\beta_D}}. \quad (16)$$

But with the assumption that the coefficients (i.e.  $k$  and  $\beta$ ) of the scaling laws are the same for each molecular weight species present (i.e. same type of polymer or chemical species in each aggregate) Eq. (16) becomes

$$M_D = \left( \frac{\sum M_i^{1-\beta} n_i}{\sum M_i n_i} \right)^{\frac{1}{\beta}}. \quad (17)$$

To extend Eq. (13) to a continuous polydisperse system the summations are simply replaced with integrals [19, 20] and so the full attenuation due to diffusion (i.e. including relaxation) is given by,

$$E = \frac{\int_0^{\infty} M_i n(M)_i \exp(R_i) \exp(-bD_i) dM}{\int_0^{\infty} M_i n(M)_i \exp(R_i) dM}. \quad (18)$$

The above equations (i.e. Eq. (10) – Eq. (18)) describe the result if only macroscopic averaging occurred but obstruction may also need to be considered [15, 18, 50]. However as discussed microscopic averaging is also observed and so the resulting attenuation measured for a polydisperse system (in size) deviates from that described by the above equations. Further difficulties arise when trying to separate summed exponential decays. A simple biexponential fit to the attenuation data for a bimodal system (i.e. only two different diffusion coefficients present) may be affected by the available signal-to-noise ratio (S/N), deviations due to instrumental error, the population fraction and amount (i.e. moles) of each of the contributing species (i.e. the amount of signal from each) and the ratio of the diffusion coefficients [51]. An exponential decay may appear multiexponential even if it is not [51]. The problems faced when accurately separating exponentials are also faced when attempting to present the data in the form of a diffusion ordered spectroscopy (DOSY) plot [7, 52-54].

#### 4. Diffusion in Restricted Systems

##### *The time-dependent diffusion coefficient*

PGSE works by spatially labelling the position of nuclear spins via magnetic field gradients and then recording the loss of phase coherence of the transverse magnetisation via spin-echoes. When this spatial label is recorded at two instants in time, the phase change becomes a function of the mean square displacement (MSD) given by Eq. (2). Eq. (2) presents the relationship between the molecular displacement due to diffusion and the diffusion equation. Importantly the MSD determined using PGSE NMR is averaged over the entire sample which need not be a disadvantage especially when working on geological samples since it is the “average” properties that are most likely of interest. For free diffusion, the length of time (i.e.,  $\Delta$ ) we choose is irrelevant in the absence of exchange and experimental complications and assuming sufficient signal exists, because the MSD scales linearly with time. In restricted systems however, the confining

boundaries can impart a signature on the MSD hence the MSD becomes a function of  $\Delta$ , the true self-diffusion coefficient  $D^0$ , and the size and shape of the confining geometry.

At short diffusion times  $\Delta \ll a^2/D^0$ , where  $a$  is the characteristic pore size, the confining geometry has little effect of the diffusing molecules therefore the MSD approaches that of free diffusion, i.e., Eq. (3). As  $\Delta$  becomes finite ( $\Delta \approx a^2/D^0$ ), a certain fraction of the particles will feel the effect of the boundary and the MSD will not scale linearly with  $\Delta$ . The apparent diffusion coefficient  $D_{app}$  determined from PGSE experiments will therefore contain information on the size and shape of the confining geometry. A relationship for the apparent diffusion coefficient can be obtained by substituting Eq. (4) for  $E(q, \Delta)$

$$D_{app}(\Delta) = -\frac{1}{\Delta} \lim_{q \rightarrow 0} \frac{\partial \ln[E(q, \Delta)]}{\partial q^2}. \quad (19)$$

It can be shown that by performing a Taylor expansion the initial decay of  $E(q, \Delta)$  with respect to  $q$  gives the MSD.  $D_{app}$  can then be written as

$$D_{app}(\Delta) = \langle (\mathbf{r}' - \mathbf{r})^2 \rangle / 2\Delta \quad (20)$$

from the low  $q$  limit of  $E(q, \Delta)$ . From Eq. (20), we can obtain a time dependant diffusion coefficient incorporating the surface to volume ratio ( $S/V$ ) of the pore [55]

$$D_{app}(\Delta) = D^0 \left( 1 - \frac{4}{9\sqrt{\pi}} \frac{S}{V} (D^0 \Delta)^{1/2} + \dots \right). \quad (21)$$

The  $S/V$  ratio is a key parameter in systems where the surface of a pore drives the chemistry (e.g., biology, catalysis, and colloidal sciences) [55]. At long diffusion times ( $\Delta \gg a^2/D^0$ ) in a totally confined pore, the maximum distance the molecules can diffuse is limited by the confining geometry thus the MSD becomes independent of  $\Delta$ . In this regime,  $D_{app}(\Delta)$  is a rich source of structural information on the confining geometry. For instance if the apparent diffusion coefficient approaches zero at long time intervals ( $D_{app}(\Delta \rightarrow \infty) \rightarrow 0$ ), it indicates the molecules are confined within the pore [55]. However in well connected pores, the time dependant diffusion coefficient approaches a finite non-zero value,  $D_{app}(\Delta \rightarrow \infty) \rightarrow D_0/\alpha$ , where  $\alpha$  is a geometrical factor known as tortuosity.

Analytical and numerical expressions to describe the PGSE NMR signal attenuation exist for molecules diffusing within simple geometries (e.g., parallel planes, sphere, and cylinder) [56-60] allowing characteristic distances in simple monodisperse systems to be determined directly from the  $q$ -space plots. Most natural systems however contain porous geometries which are complex with multiple length scales and are randomly connected. Deriving analytical expressions for such systems quickly becomes mathematically intractable hence it becomes virtually impossible to identify exact shapes. To account for these complexities, the signal attenuation expressions have been modified in some

instances to include terms which account for a distribution of characteristic distances [61, 62], however, these expressions have failed to completely describe  $E(q, \Delta)$ .

Background or internal gradients which are present within the pores can also be a significant source of uncertainty (see Section 5) or information on the confining geometry (e.g., the presence of background gradients can be used to determine the multiple length scales in porous rocks without the need to apply external gradients [63, 64]).

### 5. Suppression of Background Gradients in PGSE NMR Experiments

In NMR, the applied static magnetic field  $B_0$  (T) can never be 100% homogeneous due to two main factors: differences in magnetic susceptibility inside and/or around the NMR sample and imperfect shimming of the magnet. For inhomogeneous samples (e.g., sandstone saturated with water) the background gradients mainly result from susceptibility inhomogeneity while for homogeneous samples (e.g., water) the background gradients are primarily caused by imperfect shimming. The background gradients (also referred to as internal gradients, static gradients, and magnetic inhomogeneity) caused by susceptibility inhomogeneity may be extraordinarily strong. For example, it is estimated that red blood cells have gradients up to  $2 \times 10^{-2} \text{ T m}^{-1}$  due to the large difference in the magnetic susceptibility between the inside and outside of the cells [65, 66]; in metal hydride samples, such background gradients can be of the order of  $0.5 \text{ T m}^{-1}$  [67]; in the sandstone saturated with water, the background gradients may be as high as  $10 \text{ T m}^{-1}$ , which is  $\sim 20$  times higher than the pulsed gradient strength available on a high resolution NMR probe used in PGSE diffusion experiments. The generation of susceptibility-induced background gradients can be elaborated by the following discussion.

In a medium, the magnetic flux density  $\mathbf{B}$  (T), which is normally referred to as the magnetic field in NMR experiments, established by an applied magnetic field  $\mathbf{H}$  ( $\text{A m}^{-1}$ ) can be calculated by [68, 69]

$$\mathbf{B} = \mu_0 (1 + \chi) \mathbf{H}, \quad (22)$$

where  $\mu_0$  is the magnetic permeability of free space ( $4\pi \times 10^{-7} \text{ H m}^{-1}$ ) and  $\chi$  (dimensionless) is the magnetic susceptibility which expresses how readily the medium develops a magnetic moment on exposure to an external magnetic field.  $\chi$  is zero for vacuum and for materials it may take positive (for paramagnetic materials) or negative (for diamagnetic materials) values. A paramagnetic sample tries to pull the magnetic field into the material and thus causes a stronger magnetic field than the applied magnetic field while a diamagnetic sample tries to push the magnetic field out of the material and thus leads to a weaker magnetic field. From Eq. (22), it can be realised that spatial differences in the magnetic susceptibility results in background gradients [70].

#### *Effects of background gradients*

The diffusion induced spin-echo attenuation can be calculated via the Stejskal-Tanner equation (neglecting relaxation processes) [5],

$$\ln \left[ \frac{S^{t=acq}}{S^{t=0}} \right] = -D \int_0^t F^2(t'') dt'', \quad (23)$$

where  $F$  (rad m<sup>-1</sup>) is the spin dephasing given by

$$F(t'') = \int_0^{t''} \gamma(t') \frac{p(t')}{|p(t')|} g(t') dt' \quad (24)$$

$S^{t=acq}$  is the echo signal,  $S^{t=0}$  is the signal immediately after the first  $\pi/2$  pulse (i.e. initial excitation in the PGSE sequence),  $t$  (s) is the time at which the signal acquisition begins,  $g$  (T m<sup>-1</sup>) is the net gradient (the sum of all magnetic gradients existing in the system), and  $p$  is the selected coherence level.

Eq. (23) is evaluated over each period of a pulse sequence. For the Hahn spin-echo PGSE sequence shown in Fig. 2A, the spin-echo attenuation in the presence of background gradients is derived as

$$\begin{aligned} \ln \left[ \frac{S^{t=acq}}{S^{t=0}} \right] &= -D \left[ \int_0^{t_1} \gamma^2 \left( \int_0^{t'} (-g_0) dt' \right)^2 dt'' + \int_{t_1}^{t_1+\delta} \gamma^2 \left( \int_0^{t'} (-g_0) dt' + \int_{t_1}^{t'} (-g_0 - g_a) dt' \right)^2 dt'' \right. \\ &\quad + \dots \\ &\quad \left. + \int_{\Delta+t_1+\delta}^{2\tau} \gamma^2 \left( \int_0^{t'} (-g_0) dt' + \dots + \int_{\Delta+t_1}^{\Delta+t_1+\delta} (g_0 + g_a) dt' + \int_{\Delta+t_1+\delta}^{t'} g_0 dt' \right)^2 dt'' \right] \\ &= -\gamma^2 D \left[ \underbrace{g_a^2 \delta^2 \left( \Delta - \frac{\delta}{3} \right)}_{g_a\text{-only-term}} + \underbrace{g_a g_0 \delta \left[ 2\tau^2 - t_1^2 - t_2^2 - \delta(t_1 + t_2) - \frac{2}{3} \delta^2 \right]}_{\text{cross-term}} + \underbrace{\frac{2\tau^3}{3} g_0^2}_{g_0\text{-only-term}} \right]. \end{aligned} \quad (25)$$

Similarly for the STE-based PGSE sequence (Fig. 2B), the result is

$$\begin{aligned} \ln \left[ \frac{S^{t=acq}}{S^{t=0}} \right] &= -\gamma^2 D \left\{ \underbrace{g_a^2 \delta^2 \left( \Delta - \frac{\delta}{3} \right)}_{g_a\text{-only-term}} + \underbrace{g_0^2 \tau_1^2 \left( \tau_2 + \frac{2}{3} \tau_1 \right)}_{g_0\text{-only-term}} \right. \\ &\quad \left. + \underbrace{g_a g_0 \delta \left[ 2\tau_1 \tau_2 + 2\tau_1^2 - \frac{2}{3} \delta^2 - \delta(\delta_1 + \delta_2) - (\delta_1^2 + \delta_2^2) \right]}_{\text{cross-term}} \right\}. \end{aligned} \quad (26)$$

As shown by Eq. (25) and (26), the effects of background gradients can be classified into  $g_0$ -only-term based effects and cross-term based effects. The former only cause  $T_2$ -like signal attenuation and can be easily normalised out while the latter cannot be normalised out as they vary when  $g_a$  varies and thus can significantly hamper diffusion determination.

The effects of background gradients have been observed since the discovery of NMR. In normal one-dimensional and multi-dimensional NMR experiments, these effects are called inhomogeneous line-broadening effects in contrast with homogeneous line-broadening effects (i.e.,  $T_2$  relaxation) [8]. In diffusion-aided NMR experiments, the existence of susceptibility-induced background gradients is a double-edged sword: on one hand the background gradients convey structural information, which can be extracted by the use of special NMR techniques (e.g., [63]), and on the other hand the background gradients may significantly hamper the accurate diffusion determination using PGSE experiments (e.g., [71-74]). Below, we concentrate on how the background gradients can affect PGSE experiments deleteriously.

In most cases, the susceptibility-induced background gradients are inhomogeneous. Thus, spins inside different local structures may experience different background gradients. When the mean-squared displacement (MSD) of diffusing spins become comparable with the inhomogeneity of background gradients, the background gradients experienced by the spin ensemble will start to fluctuate through time. The effects of rapidly varying background gradients can be treated as a mechanism accelerating transverse relaxation [1, 72]. More slowly varying background gradients can be treated as a distribution  $f(g_0)$  [75], for instance, a Gaussian distribution [72]

$$f(g_0) = \exp(-g_0^2/2\sigma^2) / (2\pi\sigma^2)^{1/2}, \quad (27)$$

where  $\sigma^2$  stands for the variance of the background gradients. If it is assumed that during the diffusion time the background gradient experienced by a single spin is constant but different spins see different background gradients (NB with a distribution of  $f(g_0)$ ), the normalised echo attenuation is determined to be [72]

$$\langle \ln[E] \rangle = -(\gamma\delta g)^2 (\Delta - \delta/3) D \left[ 1 - 0.5\gamma^2 \Delta \sigma^2 D (2\tau - \Delta/2)^2 \right], \quad (28)$$

and the determined diffusion coefficient can be written as [72]

$$D' = D \left[ 1 - 0.5\gamma^2 \Delta \sigma^2 D (2\tau - \Delta/2)^2 \right]. \quad (29)$$

Based on Eq. (29), the determined diffusion coefficient (i.e., apparent diffusion coefficient) is normally smaller than the true diffusion coefficient in the presence of background gradients.

#### *Suppression of the deleterious effects of background gradients*

In 1954, Carr and Purcell developed the Carr-Purcell  $\pi$ -pulse train sequence to suppress the effects of the  $g_0$ -only-term in  $T_2$  experiments [76]. The essence of this sequence is to use a  $\pi$ -pulse train to “chop” the experimental period into small intervals so that the dephasing resulting from background gradients in one interval is cancelled by the dephasing in the subsequent interval. However, for the Carr-Purcell sequence, the calibration of the  $\pi$  pulses is critical. Meiboom and Gill [77] introduced the Carr-Purcell-Meiboom-Gill (CPMG) sequence (Fig. 4), in which the phase of the  $\pi/2$  pulse is shifted

by  $90^\circ$  relative to the phase of the  $\pi$  pulses. The spin-echo attenuation of the CPMG sequence can be written as

$$\frac{S^{t=acq}}{S^{t=0}} = \exp\left(\frac{-\gamma^2 D g_0^2 T^3}{12n^2}\right). \quad (30)$$

where  $n$  is the number of  $\pi$  pulses and  $T = 2n\tau$ . Thus, when  $n$  is large the spin-echo attenuation due to the  $g_0$ -only-term term is greatly reduced.

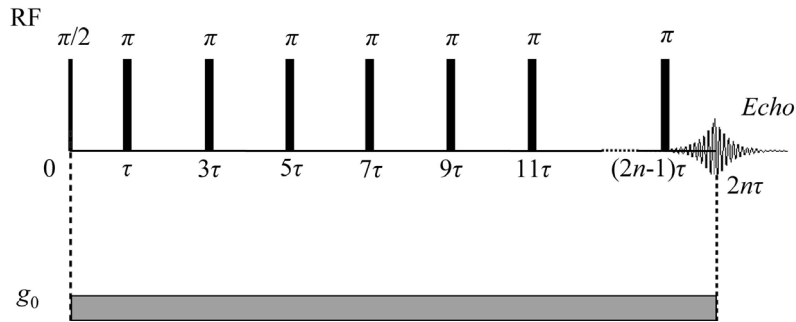


Fig. 4: The CPMG sequence in the presence of background gradients.

Various methods have been developed for the suppression of the deleterious effects of the cross-term. The most commonly used method is the so-called Cotts 13-interval sequence [71] (Fig. 5) and the normalised spin-echo attenuation for this sequence can be written as

$$E = \exp\left(-\gamma^2 D \left[ \delta^2 \left( \tau_2 + \frac{3}{4} \tau_1 - \frac{\delta}{12} \right) g^2 + \frac{1}{2} \delta \tau_1 (\delta_1 - \delta_2) g g_0 \right]\right). \quad (31)$$

Based on Eq. (31), the cross-term can be suppressed when  $\delta_1 = \delta_2$ .

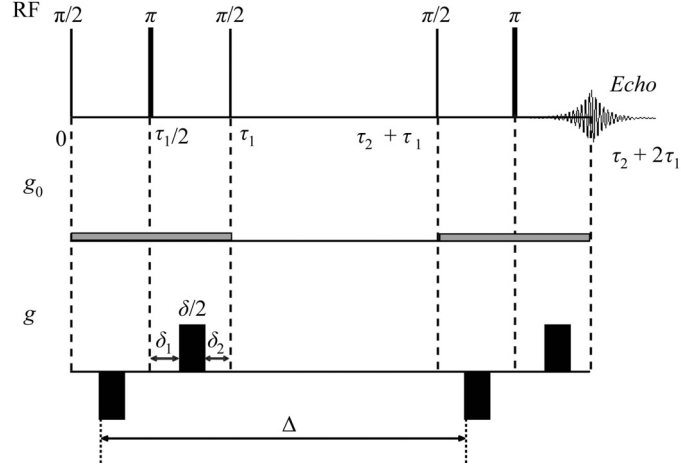


Fig. 5: The Cotts 13-interval sequence [71].

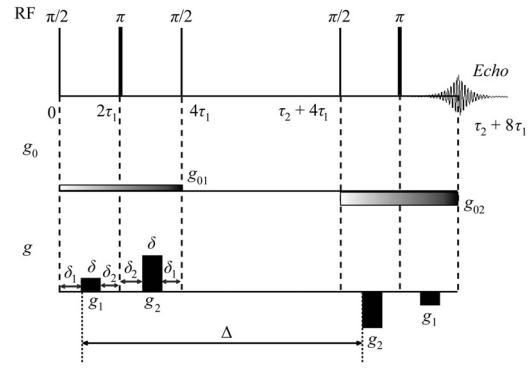
The validity of the Cotts 13-interval sequence is based on the assumption that the spin ensemble feels a constant or slightly fluctuating background gradient. However, as mentioned earlier, when the MSD of diffusing spins become comparable with the length scale of the inhomogeneity of the background gradients, the background gradient experienced by the spin ensemble starts to fluctuate through time. Therefore, new methods were developed for the suppression of the deleterious effects of non-constant background gradients ([73, 78-80]). The most recently developed methods are shown in Fig. 6. The validity of all these sequences is based on the assumption that the background gradient felt by the spin ensemble keeps constant or slightly fluctuates during the coding periods (i.e.,  $\tau_1$  periods).

For the MAG-STE sequence [78, 79], the normalised spin-echo attenuation can be written as

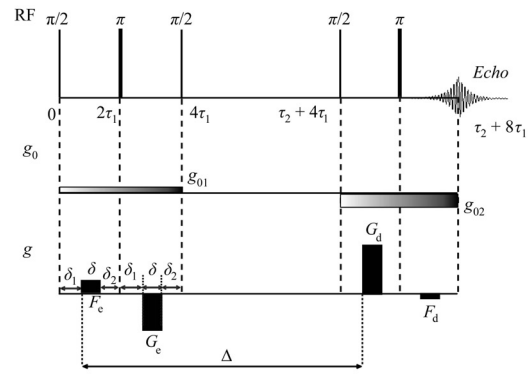
$$\begin{aligned}
 E = \exp \left\{ -\gamma^2 D \delta^2 \left[ \left( \Delta + 2\tau_1 + \delta_2 - \delta_1 - \frac{\delta}{3} \right) (g_1 - g_2)^2 \right. \right. \\
 \left. \left. + \left( 8\tau_1 + 4(\delta_2 - \delta_1) - \frac{2\delta}{3} \right) (g_1 - g_2) g_2 \right. \right. \\
 \left. \left. + \left( 4\tau_1 + 2(\delta_2 - \delta_1) - \frac{2\delta}{3} \right) g_2^2 \right] \right\}
 \end{aligned} \tag{32}$$

$$\text{when } \eta_{MAGSTE} = \frac{g_1}{g_2} = \frac{3\delta_1\delta + 3\delta_1^2 + \delta^2}{5\delta^2 + 9\delta_1\delta + 3\delta_1^2 + 12\delta_1\delta_2 + 12\delta_2\delta + 6\delta_2^2}.$$

**A**



**B**



**C**

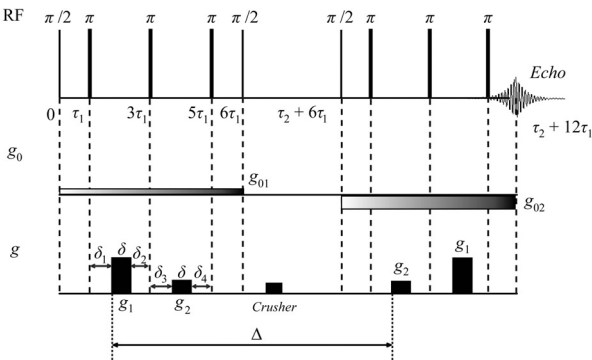


Fig. 6: (A) The MAG-STE sequence; (B) the 13-interval sequence with gradients at MPFG ratios; (C) the MAG-PGSTE sequence.

For the 13-interval sequence with gradients at magic pulsed field gradient (MPFG) ratios [73, 79], the normalised spin-echo attenuation can be written as

$$E = \exp \left\{ -\gamma^2 D \delta^2 \left[ (\tau_2 + 2\tau_1)(G_d + F_d)^2 + 2\tau_1 \left[ 2F_d^2 - (F_e + F_d)(G_e - G_d) \right] - \delta/3 \left[ G_e^2 + F_e F_d + G_d(F_e - F_d) \right] \right] \right\} \quad (33)$$

when  $F_e + G_e = F_d + G_d$ ,

$$\eta^e = \frac{G_e}{F_e} = \frac{\delta_1^2 + \delta_1 \delta + \frac{1}{3} \delta^2 - 8\tau_1^2}{\delta_1^2 + \delta_1 \delta + \frac{1}{3} \delta^2 + 2\tau_1(\delta_2 - \delta_1)}, \text{ and } \eta^d = \frac{G_d}{F_d} = 1 - \frac{8\tau_1^2 - 2\tau_1(\delta_2 - \delta_1)}{\delta_1^2 + \delta_1 \delta + \frac{1}{3} \delta^2}.$$

For the MAG-PGSTE sequence [80], the normalised spin-echo attenuation can be written as

$$E = \exp \left\{ -\gamma^2 D \delta^2 \left[ \left( \Delta + 2\tau_1 + \delta_3 - \delta_1 - \frac{\delta}{3} \right) (g_1 - g_2)^2 + \left( 8\tau_1 + 4(\delta_3 - \delta_1) - \frac{2\delta}{3} \right) (g_1 - g_2) g_2 + \left( 4\tau_1 + 2(\delta_3 - \delta_1) - \frac{2\delta}{3} \right) g_2^2 \right] \right\} \quad (34)$$

$$\text{when } \delta_1 = \delta_3 \text{ or } \delta_2 = \delta_3 \text{ and } \eta_{\text{MAG-PGSTE}} = \frac{g_2}{g_1} = \frac{3\tau_1^2 - (6\tau_1\delta_1 + 3\tau_1\delta - 3\delta_1\delta - 3\delta_1^2 - \delta^2)}{3\tau_1^2 + (6\tau_1\delta_1 + 3\tau_1\delta - 3\delta_1\delta - 3\delta_1^2 - \delta^2)}.$$

Although the sequences listed in Fig. 6 can successfully remove the cross-term resulting from non-constant background gradients, the diffusion-weighting efficiency of the gradients has been sacrificed [81]. Recently, Finsterbusch developed new suppression sequences with higher diffusion-weighting efficiency [81, 82].

## 6. Conclusions

The PGSE NMR diffusion experiment has become the method of choice for the determination of self-diffusion in complex systems due to its non-invasive nature. Physically meaningful interpretations of diffusion data from complex systems require not only starting with high-quality artifact-free experimental data but also careful consideration of the different physical phenomena which result in changes in translational motion.

## References

- [1] J. Kärgler, H. Pfeifer, W. Heink, *Adv. Magn. Reson.* 12 (1988) 1-89.
- [2] W. S. Price, *Conc. Magn. Reson.* 9 (1997) 299-336.
- [3] P. T. Callaghan, *Aust. J. Phys.* 37 (1984) 359-387.
- [4] W. S. Price, *Concepts Magn. Reson.* 10 (1998) 197-237.
- [5] E. O. Stejskal, J. E. Tanner, *J. Chem. Phys.* 42 (1965) 288-292.
- [6] P. Stilbs, *Prog. Nucl. Magn. Reson. Spectrosc.* 19 (1987) 1-45.
- [7] C. S. Johnson, Jr., *Prog. Nucl. Magn. Reson. Spectrosc.* 34 (1999) 203-256.
- [8] M. H. Levitt, *Spin Dynamics: Basics of Nuclear Magnetic Resonance*. Second ed.; Wiley, 2008.
- [9] R. Mills, *J. Phys. Chem.* 77 (1973) 685-688.
- [10] W. S. Price, *NMR Studies of Translational Motion*. In Press ed.; Cambridge University Press, 2009.
- [11] F. Bloch, *Phys. Rev.* 70 (1946) 460-474.
- [12] H. C. Torrey, *Phys. Rev.* 104 (1956) 563-565.
- [13] V. M. Kenkre, E. Fukushima, D. Sheltraw, *J. Magn. Reson.* 128 (1997) 62-69.
- [14] P. Atkins, J. De Paula, *Atkins' Physical Chemistry*. 8th ed.; W. H. Freeman, New York, 2006.
- [15] W. S. Price, F. Tsuchiya, Y. Arata, *J. Am. Chem. Soc.* 121 (1999) 11503-11512.
- [16] W. S. Price, *Annu. Rep. Prog. Chem., Sect. C: Phys. Chem.* 96 (2000) 3-53.
- [17] J. Han, J. Herzfeld, *Biophys. J.* 65 (1993) 1155-1161.
- [18] W. S. Price, *Curr. Opin. Colloid Interface Sci.* 11 (2006) 19-23.
- [19] P. T. Callaghan, D. N. Pinder, *Macromolecules* 18 (1985) 373-379.
- [20] G. Fleischer, *Polymer* 26 (1985) 1677-1682.
- [21] P. T. Callaghan, D. N. Pinder, *Macromolecules* 16 (1983) 968-973.
- [22] R. Raghavan, T. L. Maver, F. D. Blum, *Macromolecules* 20 (1987) 814-818.
- [23] W. Brown, P. Zhou, *Polymer* 31 (1990) 772-777.
- [24] W. Brown, K. Mortensen, *Macromolecules* 21 (1988) 420-425.
- [25] Q. Ying, B. Chu, *Macromolecules* 20 (1987) 362-366.
- [26] P. T. Callaghan, D. N. Pinder, *Macromolecules* 14 (1981) 1334-1340.
- [27] N. M. Ahmad, F. Heatley, P. A. Lovell, *Macromolecules* 31 (1998) 2822-2827.
- [28] T. Dobashi, F. Yeh, Q. Ying, K. Ichikawa, B. Chu, *Langmuir* 11 (1995) 4278-4282.
- [29] P. G. De Gennes, *Macromolecules* 9 (1976) 587-593.
- [30] P. G. De Gennes, *Macromolecules* 9 (1976) 594-598.
- [31] B. J. Bauer, L. J. Fetters, W. W. Graessley, N. Hadjichristidis, G. F. Quack, *Macromolecules* 22 (1989) 2337-2347.
- [32] W. Hess, *Macromolecules* 19 (1986) 1395-1404.
- [33] W. Hess, *Macromolecules* 20 (1987) 2587-2599.
- [34] I. Teraoka, *Polymer solutions: An introduction to physical properties*. Wiley, New York, 2002.
- [35] A. Sikorski, P. Romiszowski, *J. Chem. Phys.* 104 (1996) 8703-8712.
- [36] N. Clarke, F. R. Colley, S. A. Collins, L. R. Hutchings, R. L. Thompson, *Macromolecules* 39 (2006) 1290-1296.
- [37] T. Cosgrove, P. C. Griffiths, *Polymer* 36 (1995) 3335-3342.

- [38] M. D. Lechner, E. Nordmeier, D. G. Steinmeier, in: *Polymer Handbook*, 4th ed.; J. Brandrup; E. H. Immergut; E. A. Grulke; A. Abe; D. R. Bloch, (Eds.) Wiley: USA, 1999; pp VII/85 - VII/198.
- [39] G. D. J. Phillies, *Macromolecules* 19 (1986) 2367-2376.
- [40] G. D. J. Phillies, *Macromolecules* 31 (1998) 2317-2327.
- [41] G. D. J. Phillies, *Macromolecules* 35 (2002) 7414-7418.
- [42] R. A. Waggoner, F. D. Blum, J. C. Lang, *Macromolecules* 28 (1995) 2658-2664.
- [43] G. Vancso, *Eur. Polym. J.* 26 (1990) 345-348.
- [44] A. Jerschow, N. Müller, *Macromolecules* 31 (1998) 6573-6578.
- [45] M. Kurata, Y. Tsunashima, in: *Polymer Handbook*, 4th ed.; J. Brandrup; E. H. Immergut; E. A. Grulke; A. Abe; D. R. Bloch, (Eds.) Wiley: USA, 1999; pp VII/1 - VII/68.
- [46] B. R. White, G. J. Vancso, *Eur. Polym. J.* 28 (1992) 699-702.
- [47] D. W. Shortt, *J. Liq. Chromatogr.* 16 (1993) 3371-3391.
- [48] D. A. Skoog, F. J. Holler, T. A. Nieman, *Principles of Instrumental Analysis*. 5th ed.; Thompson Learning Inc., USA, 1998.
- [49] E. D. von Meerwall, *J. Magn. Reson.* 50 (1982) 409-416.
- [50] W. S. Price, F. Tsuchiya, Y. Arata, *Biophys. J.* 80 (2001) 1585-1590.
- [51] M. Nilsson, M. A. Connell, A. L. Davis, G. A. Morris, *Anal. Chem.* 78 (2006) 3040-3045.
- [52] K. F. Morris, C. S. Johnson, *J. Am. Chem. Soc.* 114 (1992) 3139-3141.
- [53] K. F. Morris, C. S. Johnson, *J. Am. Chem. Soc.* 115 (1993) 4291-4299.
- [54] P. Stilbs, *Anal. Chem.* 53 (1981) 2135-2137.
- [55] P. N. Sen, *Concepts Magn. Reson.* 23A (2004) 1-21.
- [56] J. E. Tanner, E. O. Stejskal, *J. Chem. Phys.* 49 (1968) 1768-1777.
- [57] P. T. Callaghan, *J. Magn. Reson.* 113A (1995) 53-59.
- [58] P. P. Mitra, P. N. Sen, *Phys. Rev. B: Condens. Matter* 45 (1992) 143-156.
- [59] B. Balinov, B. Jönsson, P. Linse, O. Söderman, *J. Magn. Reson.* 104A (1993) 17-25.
- [60] O. Söderman, B. Jönsson, *J. Magn. Reson.* 117A (1995) 94-97.
- [61] N. N. Yadav, W. S. Price, in: *Diffusion Fundamentals II*, S. Brandani; C. Chmelik; J. Karger; R. Volpe, (Eds.) Leipzig University Press: Berlin, 2007; pp 40-51.
- [62] D. Topgaard, O. Soderman, *Magn. Reson. Imaging* 21 (2003) 69-76.
- [63] Y.-Q. Song, S. Ryu, P. N. Sen, *Nature* 406 (2000) 178-181.
- [64] Y.-Q. Song, *Concepts Magn. Reson.* 18A (2003) 97-110.
- [65] Z. H. Endre, P. W. Kuchel, B. E. Chapman, *Biochim. Biophys. Acta* 803 (1984) 137-144.
- [66] P. W. Kuchel, B. T. Bulliman, *NMR Biomed.* 2 (1989) 151-160.
- [67] W. D. Williams, E. F. W. Seymour, R. M. Cotts, *J. Magn. Reson.* 31 (1978) 271-282.
- [68] B. I. Bleaney, B. Bleaney, *Electricity and magnetism*. Oxford University Press, London, 1976.
- [69] E. M. Purcell, *Electricity and magnetism*. 2nd ed.; McGraw-Hill Book Co, New York, 1985.

- [70] P. W. Kuchel, B. E. Chapman, W. A. Bubb, P. E. Hansen, C. J. Durrant, M. P. Hertzberg, *Concepts Magn. Reson.* 18A (2003) 56-71.
- [71] R. M. Cotts, M. J. R. Hoch, T. Sun, J. T. Markert, *J. Magn. Reson.* 83 (1989) 252-266.
- [72] J. H. Zhong, J. C. Gore, *Magn. Reson. Med.* 19 (1991) 276-284.
- [73] P. Galvosas, F. Stallmach, J. Kärgler, *J. Magn. Reson.* 166 (2004) 164-173.
- [74] F. Stallmach, P. Galvosas, *Annu. Rep. NMR Spectrosc.* 61 (2007) 51-131.
- [75] I. Zupančič, *Solid State Commun.* 65 (1988) 199-200.
- [76] H. Y. Carr, E. M. Purcell, *Phys. Rev.* 94 (1954) 630-638.
- [77] S. Meiboom, D. Gill, *Rev. Sci. Instrum.* 29 (1958) 688-691.
- [78] P. Z. Sun, J. G. Seland, D. Cory, *J. Magn. Reson.* 161 (2003) 168-173.
- [79] P. Galvosas. PFG NMR-Diffusionsuntersuchungen mit ultra-hohen gepulsten magnetischen feldgradienten an mikroporösen materialien. PhD Thesis, Universität Leipzig, 2003.
- [80] G. Zheng, W. S. Price, *J. Magn. Reson.* 195 (2008) 40-44.
- [81] J. Finsterbusch, *J. Magn. Reson.* 191 (2008) 282-290.
- [82] J. Finsterbusch, *J. Magn. Reson.* 193 (2008) 41-48.